Molecular dynamics simulations of surfactant and nanoparticle self-assembly at liquid–liquid interfaces

2007 J. Phys.: Condens. Matter 19 375109

(http://iopscience.iop.org/0953-8984/19/37/375109)

IOP PUBLISHING JOURNAL OF PHYSICS: CONDENSED MATTER

J. Phys.: Condens. Matter **19** (2007) 375109 (14pp) doi:10.1088/0953-8984/19/37/375109

Molecular dynamics simulations of surfactant and nanoparticle self-assembly at liquid–liquid interfaces

Mingxiang Luo and Lenore L Dai

Department of Chemical Engineering, Texas Tech University, Lubbock, TX 79409, USA

Received 13 December 2006
Published 13 August 2007
Online at stacks.iop.org/JPhysCM/19/375109

Abstract

We have performed molecular dynamics (MD) simulations to investigate self-assembly at water–trichloroethylene (TCE) interfaces with the emphasis on systems containing modified hydrocarbon nanoparticles (1.2 nm in diameter) and sodium dodecyl sulfate (SDS) surfactants. The nanoparticles and surfactants were first distributed randomly in the water phase. The MD simulations have clearly shown the progress of migration and final equilibrium of the SDS molecules at the water–TCE interfaces with the nanoparticles either at or in the vicinity of the interfaces. One unique feature is the 'attachment' of surfactant molecules to the nanoparticle clusters in the water phase followed by the 'detachment' at the water–TCE interfaces. At low concentrations of surfactants, the surfactants and nanoparticles co-equilibrate at the interfaces. However, the surfactants, at high concentrations, competitively dominate the interfaces and deplete nanoparticles away from the interfaces. The interfacial properties, such as interfacial thickness and interfacial tension, are significantly influenced by the presence of the surfactants, but not the nanoparticles. The order of the surfactants at the interfaces increases with increasing surfactant concentration, but is independent of nanoparticle concentration. Finally, the simulation has shown that surfactants can aggregate along the water–TCE interfaces, with and without the presence of nanoparticles.

(Some figures in this article are in colour only in the electronic version)

Self-assembly of nanosized objects at liquid–liquid interfaces is of tremendous interest for various natural and industrial applications. For example, self-assembly of surfactant molecules or polymers at liquid–liquid interfaces is essential in the preparation and stabilization of conventional emulsions. The importance of conventional emulsions is reflected through their wide applications in the food, cosmetic, pharmaceutical, petroleum, fine chemical, and coating industries. Surfactant interfacial self-assembly is also critical in numerous processes such as lubrication, detergency, biological transferring, and polymer processing. Recently, there has been a growing interest in the self-assembly of nanoparticles due to their important applications. For example, self-assembled nanoparticles at a liquid–liquid interface serve as building blocks

for bottom-up assembly of new functional materials with unique physical properties [1, 2]. Furthermore, there is growing interest in solid-stabilized emulsions that use solid nanoparticles or microparticles as emulsion stabilizers. For these systems, the self-assembly of solid particles at liquid–liquid interfaces is essential [3–12]. Although the fundamentals of surfactant adsorption at liquid–liquid interfaces are well understood, the self-assembly of nanoparticles at liquid–liquid interfaces has not been fully explored. One of the remaining challenges is to understand multiphase interactions, self-assembly processes, and self-assembled structures of nanoparticles, especially when the size of the nanoparticles is comparable with the molecular dimension of the surrounding liquids. Dai *et al* [12] have reported the success of using solid-stabilized emulsions as a new experimental model system to investigate the detailed self-assembled structure of nanoparticles (1–5 nm) at a water–trichloroethylene (TCE) interface. This assembly was determined by use of an environmental transmission electron microscope (E-TEM). In sharp contrast to microparticles or large-size nanoparticles forming a monolayer at liquid–liquid interfaces, ultra small dodecanethiol-capped nanoparticles of 1–5 nm form randomly distributed multilayers at the water–TCE interfaces, with an interparticle distance varying from close contact to approximately 25 nm [12]. This interesting result offers the first direct observation of nanoparticles in a liquid medium using E-TEM and opens new opportunities for high-resolution nanoparticle research involving liquids. However, the microscopy work is limited to probing the equilibrium structure, not the dynamic self-assembly process. In addition, the experimental images do not provide detailed information of interfacial properties such as the interfacial thickness or chemical composition. Recently, Luo *et al* [13] have presented the molecular dynamics (MD) simulation results of the *in situ* self-assembly of modified hydrocarbon nanoparticles with mean diameters of 1.2 nm at water–TCE interfaces. The simulation has clearly shown the progress of cluster formation, migration, and final equilibrium of both single particles and clusters at liquid–liquid interfaces. In addition, the simulation shows that the water–TCE interfacial thickness analyzed from density profiles is influenced by the presence of nanoparticles either near or in contact with the interface but is independent of the number of nanoparticles present [13].

One fundamental as well as practical question has not been addressed is the heterogeneous or competitive self-assembly of nanoparticles and surfactants at liquid–liquid interfaces for systems containing a mixture of surfactants and nanoparticles. The application of surfactants is ubiquitous, ranging from natural and industrial processes to commercial and personal care products. However, many processes are performed in the presence of both nanoparticles and surfactants. For example, surfactants are widely used in the chemical flooding processes in tertiary (enhanced) oil recovery. The surfactant concentration can be low (0.1–0.2%) or high (2.0–10.0%) depending on the application [14]. Based on the principles of solid-stabilized emulsions, nanoparticles in the oil well, such as clays, scales, and corrosion products can also self-assemble at the oil–water interfaces [15]; thus the heterogeneous or competitive adsorption between solid particles and surfactants is important. As another example, in a multi-layer coating process, the competition between surfactants (often for wetting purpose) and nanoparticles (often for property enhancer purpose) at liquid–liquid interfaces is also not negligible. Here we will report MD simulations on the self-assembly at liquid–liquid interfaces when the systems contain a mixture of surfactants and nanoparticles.

MD simulation is a powerful tool for obtaining molecularly detailed information and the underlying physics of various systems, including liquid–liquid interfaces [16], liquid–liquid interfaces containing surfactant molecules [16], and liquid–liquid interfaces containing nanoparticles [13]. For example, MD simulations have been successfully performed on water–carbon tetrachloride (CCl_4) [17, 18], water–octane [19], water–decane [20], water–dichloroethane [21, 22], and water–dichloromethane [23] interfaces. These simulations

have provided molecular information that supplements experimental capabilities and have illuminated new underlying physics. Moreira and Skaf [17] found a significant reduction of hydrogen bonds near the water–carbon tetrachloride interface and the dipole moments of water showed preference of aligning along the interface. The work by Zhang *et al* [18] suggests there are inner and outer layers near the water–octane interface, and that the water dipoles point in opposite directions at the different layers. Benjamin [22] investigated the self-diffusion of liquid molecules at water–dichloroethane interfaces and found that the diffusion of both water and dichloroethane molecules was faster parallel to the interface than perpendicular to it. The MD simulations have also been extended to liquid–liquid interfaces containing surfactant molecules. Recently, Rivera *et al* [24] simulated water–alkane systems containing methanol and reported the surfactant behavior of methanol, i.e. methanol molecules adsorb preferably at the water–alkane interface and decrease the interfacial tension through molecular rearrangement. Schweighofer *et al* [25] observed the inclination of sodium dodecyl sulfate (SDS) anionic surfactants at water–CCl_4 interfaces. The mixture of SDS with nonionic surfactants was simulated by Dominguez [26] and the results showed that the interaction and charge distribution had significant effects on the location of surfactants. Finally, as discussed previously, Luo *et al* [13] have successfully simulated the *in situ* self-assembly of modified hydrocarbon nanoparticles at a water–TCE interface. In this paper, we report the MD simulations investigating the self-assembly at liquid–liquid interfaces with the presence of both surfactants and nanoparticles. We will address the following fundamental questions: (i) if the surfactants and nanoparticles are initially distributed randomly in one of the bulk phases, what are their equilibrium locations? (ii) will they assemble heterogeneously at the same liquid–liquid interface or be competitive to each other? (iii) what are the influences of surfactants and nanoparticles on interfacial properties? (iv) what are the structure and distribution of surfactants and nanoparticles at the molecular level?

1. Methodology

The MD simulations were performed using the GROMACS 3.3.1 package [27–30]. The interaction parameters were computed using the GROMOS96 force field [31], with the intermolecular (non-bonded) potential represented as a sum of the Lennard-Jones (LJ) force and pairwise Coulomb interaction and the long-range electrostatic force determined by the cut-off method. The velocity Verlet algorithm was used for the numerical integrations [32], and the initial atomic velocities were generated with a Maxwellian distribution at the given absolute temperature [33, 34].

Water was modeled using the single point charge (SPC) model [35, 36]. The structures and topologies of sodium dodecyl sulfate (SDS) and trichloroethylene (TCE) were generated by the small-molecule topology generator PRODRG [37]. The spherical modified hydrocarbon nanoparticle (mean diameter of 1.2 nm) was truncated from a diamond-like lattice made of carbon atoms that bonded in non-planar hexagonal structure and, to increase the simulation efficiency, saturated with united CH, CH_2, and CH_3 atoms [13, 38]. We have simulated four types of systems detailed as follows: system A was a 20 ns simulation of pure water and TCE; systems B were 50 ns simulations of water and TCE containing 5 and 10 nanoparticles, respectively; systems C were 50 ns simulations of water and TCE containing 5, 10, 20, 50, and 99 SDS molecules, respectively; systems D were 50 ns simulations of water and TCE containing 2, 5 and 10 nanoparticles, and different numbers of SDS molecules, respectively. Nanoparticles or SDS molecules were added into the water phase at the beginning of the simulations for systems B or C. The surfactants were added into the water phase after the nanoparticles' initial insertion at the beginning of the simulations for systems D. It is

Table 1. Composition of the simulation systems.

System	Nanoparticle (particle)	SDS (molecule)	TCE (molecule)	Water (molecule)	Runs[a]
A	0	0	288	1 491	4
B1	5	0	5249	33 971	8
B2	10	0	4500	23 585	6
C1	0	5	4500	23 585	4
C2	0	10	5249	33 059	4
C3	0	20	5249	32 888	4
C4	0	50	5249	32 361	4
C5	0	99	5249	30 924	4
D1	2	5	5249	33 183	4
D2	5	10	5249	32 755	4
D3	5	20	5249	32 582	4
D4	5	50	5249	32 058	8
D5	5	99	5249	30 924	4
D6	10	20	5249	32 281	4
D7	10	50	5249	31 757	8
D8	10	99	5249	30 924	8

[a] Number of parallel runs with different initial velocities from Maxwellian distribution. System A simulates 20 ns and the other systems simulate 50 ns.

worthwhile noting that our approach is different from several other MD simulations [25, 26, 39] of liquid–liquid interfaces containing surfactants only, where the surfactants are initially pinned at the interfaces. In our simulations, the surfactants, as well as nanoparticles, were initially added into the water phase to empower the simulation to compute their dynamics in the two phases and final equilibrium positions. System A contains a total of 5913 atoms and the initial size of the simulation box is $3.3 \times 3.3 \times 7.8$ nm^3. The initial size of the simulation box was $8.3 \times 8.3 \times 19.6$ nm^3 for systems B and $10.4 \times 10.4 \times 20.6$ nm^3 for systems C and D. The atom numbers are different in systems B, C, and D due to the presence of different numbers of nanoparticles and surfactant molecules. A summary of the computed systems is shown in table 1. All systems lead to an initial density of 1.0 g cm^{-3} for water and 1.456 g cm^{-3} for TCE. After the construction of the simulation box, the energy was minimized using the steepest descent method with a cutoff of 10 Å for van der Waals and Coulomb forces. Simulations were performed in NPT (constant number of molecules, constant pressure, and constant temperature) ensemble [40] using the Berendsen thermostat [41] with coupled temperature and pressure at 300 K and 1 bar. We used a 9 Å cut-off for van der Waals interactions and a 10 Å cut-off for long-range electrostatics for systems C and D. Periodic boundary conditions were applied in all directions. The time step was 4 fs. The results were averaged from multiple parallel runs. The simulation details of systems A and B can be found in the previously published paper by Luo *et al* [13]. After the simulation, the interfacial properties and structures were characterized using the GROMACS analysis tools and visual molecular dynamics (VMD) [42].

2. Results and discussion

2.1. In situ self-assembly of surfactants and nanoparticles at water–TCE interfaces

The emphasis here is investigating the interfacial self-assembly of systems containing a mixture of surfactants and nanoparticles; for comparison, we have also included systems

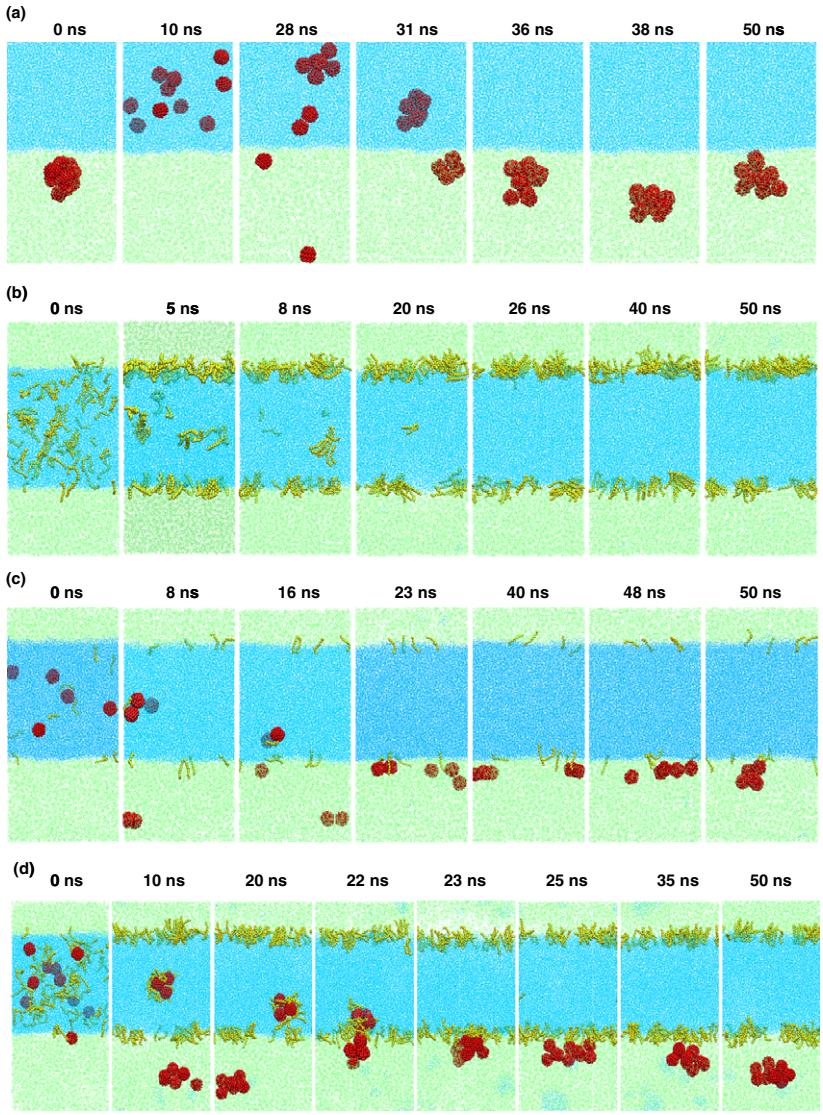

Figure 1. Sample snapshots of systems (a) B2, (b) C5, (c) D2, and (d) D8 at different simulation time intervals. The nanoparticles, SDS molecules, water phase and TCE phase are represented by red spheres, in yellow chains, in blue (dark phase), and in lime (light phase), respectively.

involving surfactants or nanoparticles only. Figure 1(a) shows the progress of cluster formation, migration, and final equilibrium of 10 nanoparticles (B2) at the water–TCE interfaces. Similar *in situ* self-assembly of a system containing 99 surfactants (C5) is shown in figure 1(b). It is noticeable that the surfactants equilibrate at the water–TCE interfaces at a much faster rate compared to that of nanoparticles. Interestingly, it becomes more complicated with the presence of both surfactants and nanoparticles in systems D. At low surfactant concentrations (D1–D4 and D6–D7), the surfactants and nanoparticles can co-equilibrate at the same liquid–liquid interfaces, as demonstrated in an example in figure 1(c). However, at the highest surfactant concentration when the systems contain 99 surfactants, the nanoparticles are depleted away

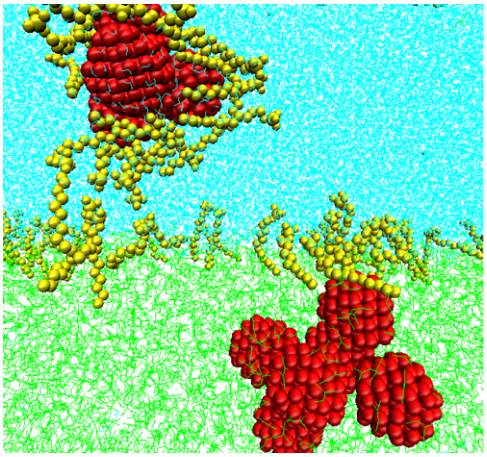

Figure 2. Snapshot of one sample run of system D8 at 21 ns. Four nanoparticles form a cluster in water and six nanoparticles form a cluster in TCE. The nanoparticles, SDS molecules, water phase and TCE phase are represented by red spheres, in yellow, in blue (top), and in lime (bottom), respectively.

from the interface at equilibrium (figure 1(d)). This is most likely due to the steric effect of surfactants, although a more detailed mechanism needs to be further explored.

It is important to note the observed 'attachment' and 'detachment' of surfactants to nanoparticles when the systems contain both surfactants and nanoparticles. In all simulated systems, the surfactants can attach to the nanoparticles and diffuse simultaneously with the nanoparticles in the water phase towards the interfaces. Upon reaching the water–TCE interface, the surfactants will detach themselves from the nanoparticles and remain at the interfaces, whereas the nanoparticle clusters will diffuse into the TCE phase. The nanoparticle clusters will finally equilibrate at the water–TCE interfaces except in the systems containing 99 surfactants, as discussed previously. Figure 2 is a snapshot of one sample run of system D8 at 21 ns when two nanoparticle clusters are in the vicinity of a water–TCE interface. The upper nanoparticle cluster surrounded by surfactants is approaching the interface and the lower nanoparticle cluster has been depleted away from the interface. When the surfactants are in contact with nanoparticles, the hydrophobic tails of the SDS molecules orient closer to the nanoparticle surfaces with the hydrophilic heads pointing outwards, as shown in figure 3. This is mainly due to the hydrophobic nature of the nanoparticles, the hydrophilic nature of the surrounding water phase, and the amphiphilic nature of the SDS molecules.

2.2. Influences of surfactants and nanoparticles on interfacial thickness and interfacial tension

Interfacial thickness is an important interfacial physical property that is barely obtainable experimentally but only theoretically or computationally. One intuitive question to ask here is about the influences of surfactant and nanoparticle mixtures on interfacial thickness. Figure 4(a) presents the mass density profile of a pure water–TCE system (system A) and figures 4(b)–(e) are those of systems containing nanoparticles (system B2), or surfactants (system C5), or both (systems D2 and D8). Interfacial thickness, defined as the distance over which the TCE density drops from 90% to 10% of the bulk density, is plotted as a function of number of SDS surfactants in figure 5. It illustrates a monotonic increase of the interfacial thickness with increasing number of SDS surfactants. Luo *et al* [13] have shown that the water–TCE interface thickness is increased by approximately 40% with the presence

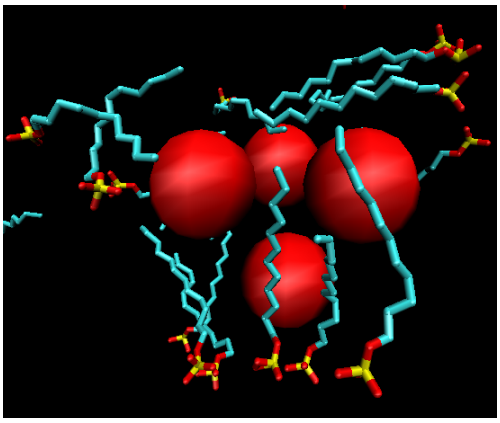

Figure 3. Snapshot of one sample run of system D8 at 10 ns. Four nanoparticles form a cluster in water and are represented as simplified red balls. The hydrophobic chains of SDS molecules are represented in blue and the hydrophilic head groups of SDS molecules are represented in red and yellow.

of nanoparticle clusters either near or in contact with the interface but is independent of the number of nanoparticles present. Figure 5 illustrates that nanoparticles may also influence the interfacial thickness but their effect is significantly less compared to that of surfactants. The strong influence of SDS surfactants on interfacial thickness is also observed by the MD simulation by Schweighofer *et al* [25] in which they studied the SDS at water–CCl_4 interfaces, although the latter involves surfactants only. Recently, Li *et al* [43] have reported that the dodecane–water interfacial thickness increases with increasing the concentrations of linear alkanesulfonate and alkybenzenefulonates using a dissipative particle dynamics simulation. According to the theoretical work by Telo da Gama *et al* [44], the increased interfacial thickness is due to the accommodation of the presence of concentrated surfactants at the interface.

Another important physical property is interfacial tension (γ), which is calculated using

$$\gamma = \frac{1}{2}\left\langle L_z\left(p_{zz} - \frac{p_{xx} + p_{yy}}{2}\right)\right\rangle \tag{1}$$

where $p_{\alpha\alpha}$ ($\alpha = x, y,$ or z) is the $\alpha\alpha$ element of the pressure tensor and L_z is the linear dimension of the simulation cell in the z direction perpendicular to the interfaces [19, 24, 34]. Figure 6 shows the normalised water–TCE interfacial tension as a function of the number of SDS molecules in systems C and D. The interfacial tension is normalised by dividing the interfacial tension of each system with the interfacial tension of pure water–TCE. The pure water–TCE interfacial tension, simulated from system A, is 41.5 mN m^{-1}, which is reasonably close to the experimental value of 38.9 mN m^{-1} measured in our laboratory using a Krüss K100 tensiometer. Figure 6 shows that the increasing number of SDS molecules results in a significant reduction of interfacial tension. The reduction slows down at higher SDS concentrations. It is noticeable that here nanoparticles have a minor influence on interfacial tension, which is consistent with the observation on systems B. Surfactants such as SDS molecules are well known for effective reduction of interfacial tensions.

A similar reduction has been observed in the MD simulations of water–vapor and water–CCl_4 interfaces containing surfactants [45]. The reduction of surfactants on interfacial tension has also been studied extensively from experimental and practical aspects. One prevailing mechanism has been proposed by Langmuir in which the reduction of surface tension is equivalent to the pressure of the two-dimensional surfactant film [46]. The theoretical work

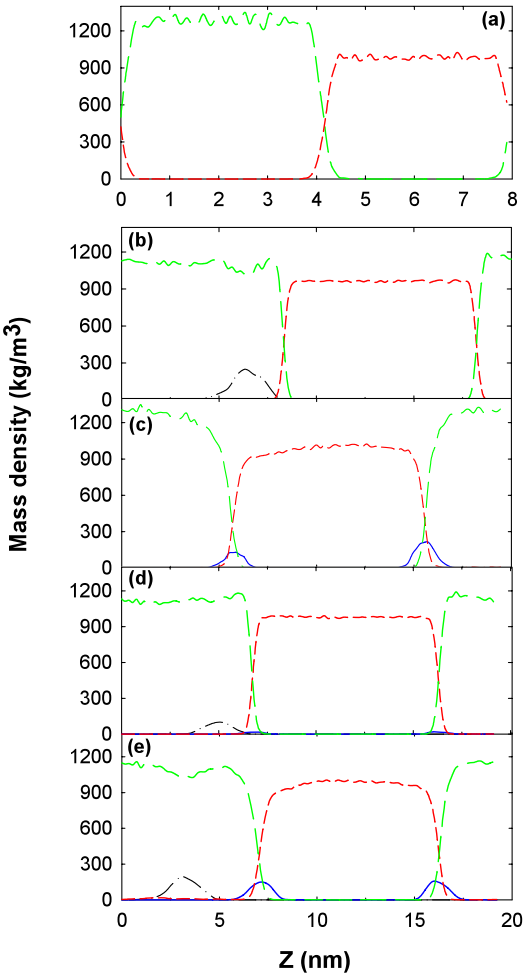

Figure 4. Mass density profiles for systems (a) A, (b) B2, (c) C5, (d) D2, and (e) D8 obtained by dividing the simulation cell into 100 slabs parallel to the water–TCE interface. Densities were averaged over the last 1 ns. The nanoparticles, SDS, water, and TCE molecules are represented in black, blue, red, and green, respectively.

by Telo da Gama *et al* [44] used a generalized van der Waals model and suggested that 'the reduction in surface tension is proportional to adsorbed surfactants only at low concentration' but the correlation fails at high interfacial surfactant concentrations. In contrast, there is sparse work on the effect of nanoparticles on interfacial tension. Recently, Ravera *et al* [47] have reported the experimental work on the influence of colloidal silica nanoparticles on interfacial tensions of water–air and water–hexane interfaces containing hexadecyltrimethylammonium bromide (CTAB) surfactant using a drop shape tensiometer. Their work has shown that the presence of 1 wt% nanoparticles significantly reduces the effectiveness of CTAB due to the adsorption of surfactants onto nanoparticles and leads to a reduction of surfactant concentration at the interface. Here we have used nanoparticles (1.2 nm in diameter) that are more than a magnitude smaller than those in the experimental work. In addition, the simulation has clearly shown that although the SDS surfactants attach to the nanoparticles in the water phase, they detach themselves when reaching the interface and remain finally in equilibration at the

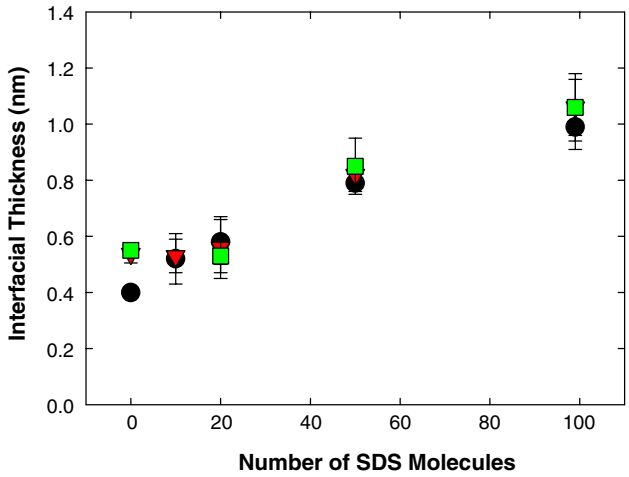

Figure 5. Interfacial thickness as a function of the number of SDS molecules. The circles, triangles, and squares represent interfacial thicknesses of the systems without nanoparticles and with five and ten nanoparticles, respectively.

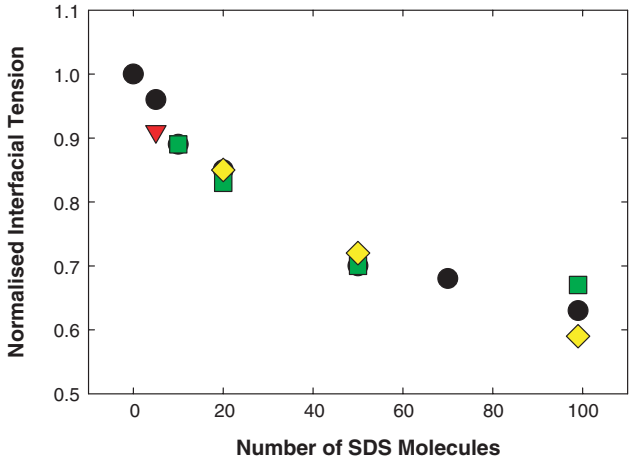

Figure 6. Normalised water–TCE interfacial tensions as a function of the number of surfactant molecules. The circles, triangles, squares, and diamonds represent interfacial tensions of the systems without the nanoparticles and with two, five, and ten nanoparticles, respectively.

interfaces. We hypothesize that the minor effect of nanoparticle clusters on interfacial tension here may also be explained by their small contact area with the interface (only one or two particles within the clusters are 'truly' in contact with the interface) thus the effect on interfacial pressure is less significant.

2.3. Conformation and lateral distribution of surfactants at liquid–liquid interfaces

One advantage that the simulation provides is the detailed structural information at the molecular level. Our simulation has shown the anionic head groups (SO_4^-) of the SDS molecules immersed in the water phase with the tail groups (hydrocarbon chains) stretching across the interface into the TCE phase. In other words, the surfactants span across the

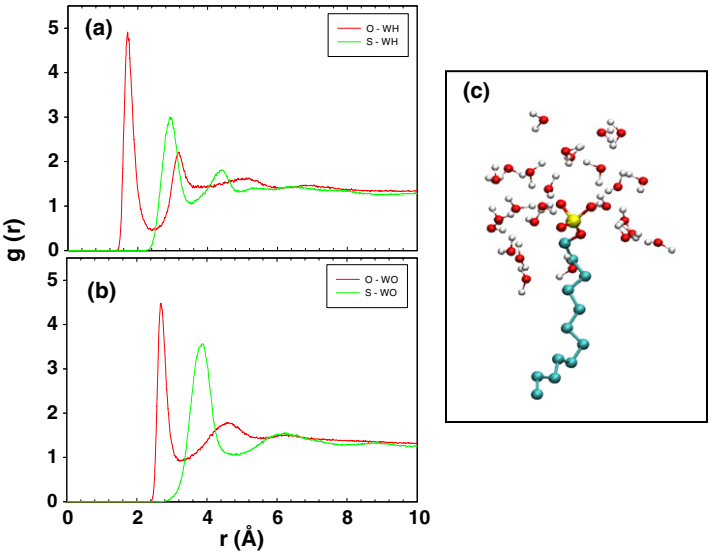

Figure 7. SDS's head group-water radial distribution functions for system D8. (a) Correlations involving the water hydrogen atoms. (b) Correlations involving the water oxygen atoms. The red and green lines refer to the $g(r)$ calculated with the sulfur and oxygen atoms of the head groups of SDS, respectively. Data are averaged over eight runs within the last 5 ns. (c) One isolated SDS molecule from the simulation to show the preference of the hydrogen atoms (in white spheres) in water to the SDS head group.

water–TCE interface microscopically. This is due to the hydrophilic and hydrophobic nature of their head and tail groups, respectively. Figure 7 shows the head group-water radial distribution functions for system D8. Four types of correlations were calculated: $g(r_{\mathrm{O-WH}})$, $g(r_{\mathrm{S-WH}})$, $g(r_{\mathrm{O-WO}})$, and $g(r_{\mathrm{S-WO}})$. The subscript symbols 'O' and 'S' refer to the oxygen and sulfur atoms in SDS, and 'WH' and 'WO' refer to the hydrogen and oxygen atoms in water. Figure 7(a) is the correlation between the anionic SDS head group and the hydrogen atoms in water and figure 7(b) shows those with the oxygen atom in water. Figure 7 shows that the hydrogen atoms in water align closer to the head group of the SDS molecule, as demonstrated by first peaks of $g(r_{\mathrm{O-WH}})$ at 1.7 Å and $g(r_{\mathrm{S-WH}})$ at 2.9 Å. Both first peaks occur at shorter distances compared to those of $g(r_{\mathrm{O-WO}})$ at 2.7 Å and $g(r_{\mathrm{S-WO}})$ at 3.8 Å, respectively. An isolated SDS molecule from the MD simulation is shown in figure 7(c) to illustrate the preferable orientation of the water molecules. Such observations are consistent with the work by Schweighofer *et al* [38] on SDS at water–vapor and water–CCl_4 interfaces.

Another fundamental question of interest is the potential ordering of the SDS surfactants at water–TCE interfaces. The ordering of the surfactants is often characterized by a deuterium order parameter (S_{CD}), which is 'the average inclination of the C–D bond with respect to surface normal' [39]. The deuterium order parameter originates from the nuclear magnetic resonance (NMR) experiments on lipid bilayers in which the hydrogen atoms are replaced by deuterium atoms [48]. The deuterium order parameter can be calculated following [48],

$$S_{\mathrm{CD}} = \tfrac{1}{2}\langle 3\cos^2\theta_{\mathrm{CD}} - 1\rangle \qquad (2)$$

where θ_{CD} is the angle between the interface normal and the molecular axis of the surfactant. The two extremes of the deuterium order parameters are 1 and $-1/2$, corresponding to a perfect order along the interface normal and a perfect order along the interface. The value equals zero if the surfactants pack isotropically at the interface.

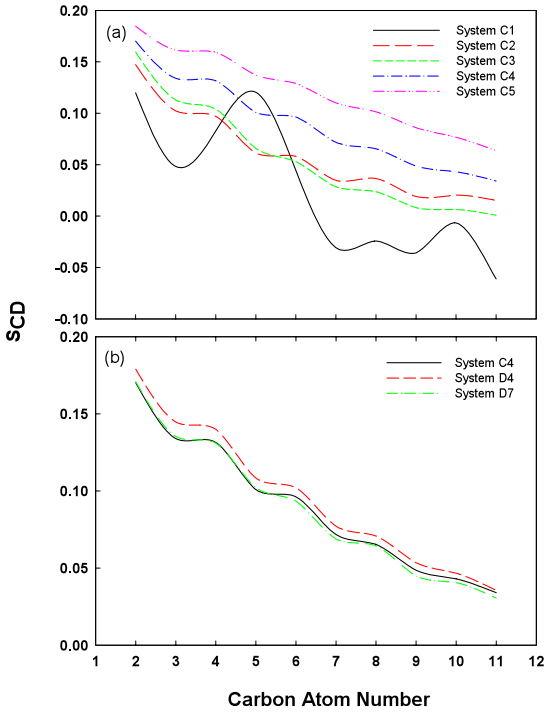

Figure 8. The deuterium order parameter (S_{CD}) as a function of carbon atom number starting '2' for the carbon atom adjacent to the head group. (a) Influence of SDS concentration; (b) influence of nanoparticle concentration.

Figure 8 plots the influence of surfactant and nanoparticle concentration on the deuterium order parameter of the SDS tail chain. As illustrated in figure 8(a), the order parameter decreases for the carbon atoms further away from the head group which indicates more flexibility toward the tail end. However, S_{CD} increases with increasing SDS concentration thus suggesting that SDS carbon chains become more ordered along the interfacial normal at higher SDS concentrations. In particular, we notice that the order parameter of system C1 is more disordered and abnormal compared to the other systems. This may be explained by the fact that the interface is nearly empty and the surfactants have more freedom to arrange themselves. Another possibility is due to the small sample size (only five SDS molecules presented) which leads to a poor statistical average. The increased ordering as a function of increasing surfactant concentration has been observed in other simulations [26, 43, 49] and experiments [50, 51]. Surprisingly, the order parameter is not influenced by the presence of nanoparticles (either at the interface or in the vicinity of the interface), as shown in figure 8(b). This may be again hypothesized by the fact that the nanoparticle clusters only have one or two particles in contact with the interface. In addition, the interface is still relatively empty. For systems C and D containing 99 surfactants, the average interfacial area is 210 $Å^2$/molecule, which is significantly higher than the saturation value of 59 $Å^2$/molecule for a monolayer of SDS at water–CCl_4 interfaces [26]. The high surface area per molecule may also explain why no consistent tile angle of surfactants is observed in systems C and D other than the potential solvent contribution. For comparison, it has been reported that SDS molecules, at a surface coverage of 45 $Å^2$/molecule, have an average tile angle of 40° relative to the surface normal direction at a water–CCl_4 interface [25].

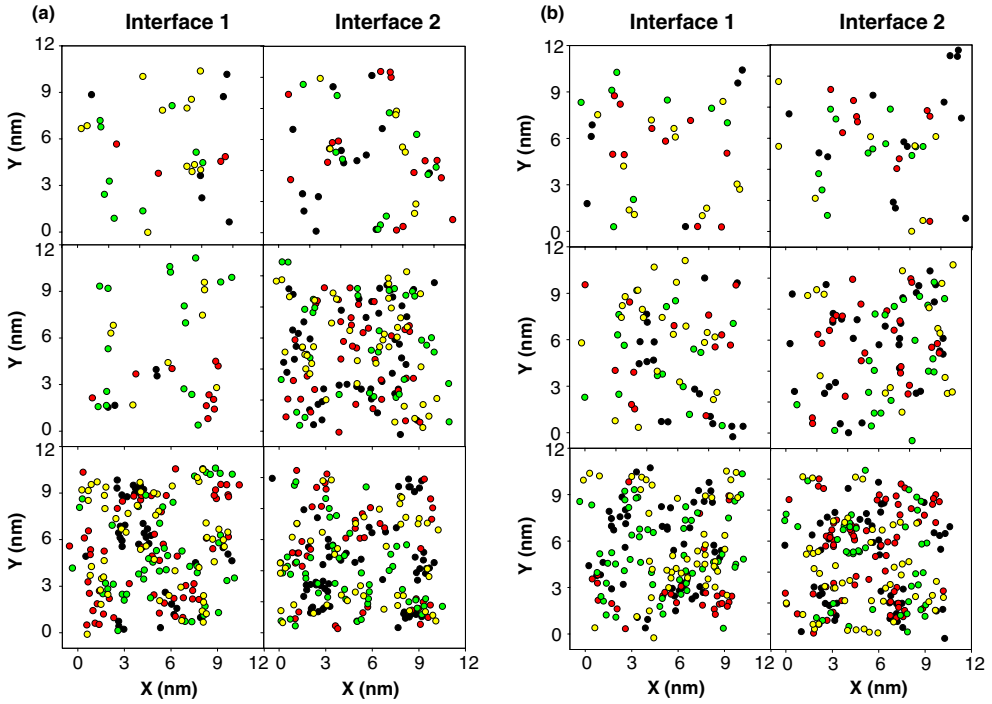

Figure 9. Lateral distribution of SDS molecules at water–TCE interfaces. Each point represents the center of mass of a SDS molecule. Parallel runs are represented in different colors. Panels from top to bottom are systems containing 20, 50, and 99 surfactants, respectively. (a) Systems without nanoparticles, C3, C4, and C5. (b) Systems with nanoparticles, D6, D7, and D8.

We have also evaluated the lateral distribution of SDS surfactants at water–TCE interfaces. As discussed above, the simulation has shown that the surfactants are always equilibrated at the water–TCE interfaces. An intriguing observation is the aggregation of the surfactants, especially when the interface has high surfactant concentrations. Figure 9(a) shows the lateral location (center of mass) of the SDS molecules at each interface, including parallel runs of systems C3 (top panels), C4 (middle panels), and C5 (bottom panels). Different colors here represent the parallel runs for each system. The size of the circles shows the cross area of the SDS molecules. It is obvious that the degree of aggregation increases with the surfactant concentration. For system C5, a majority of SDS surfactants aggregate into different size of clusters, some of which overlap each other and form closely packed clusters. Although aggregation of surfactants sometimes initiates in the water phase, it mostly occurs after the surfactant's migration to the interface. The MD simulation work by Nicolas [52] and van Buuren *et al* [53] has shown significant motion of surfactin molecules at a water–hexane interface and surfactant mixtures at a diglyceride–water interface, respectively. Here the SDS molecules also diffuse along the interface (data not shown) which probably leads to cluster formation due to 'attractive van der Waals interactions between the tails' [54]. It is also worthwhile to note that interfacial aggregation of surfactants contradicts the statement by Li *et al* [43] that surfactant molecules do not have lateral interactions at low concentrations. Finally, we discuss the influence of nanoparticles on the aggregation of surfactants. Surprisingly, the presence of nanoparticles, either at or in the vicinity of the interface, does not significantly alter the aggregation of surfactants, as qualitatively shown in figure 9(b).

3. Conclusion

Molecular dynamics simulations have been performed to investigate the self-assembly at water–TCE interfaces with the focus on systems containing modified hydrocarbon nanoparticles and SDS surfactant molecules. To the best of our knowledge, this work provides the first molecular dynamics simulation of the *in situ* interfacial self-assembly when a system contains both nanoparticles and surfactants. The simulation has clearly shown the progress of migration and final equilibrium of SDS molecules at the liquid–liquid interfaces with the nanoparticles either at or in the vicinity of the interface. One unique feature is the 'attachment' of surfactant molecules to the nanoparticles clusters in the water phase followed by the 'detachment' at the water–TCE interface. At low concentrations of surfactants, the surfactants and nanoparticles co-equilibrate at the interfaces. However, the surfactants, at high concentrations, competitively dominate the interface and deplete nanoparticles away from the interfaces. The interfacial properties, such as interfacial thickness and interfacial tension, are significantly influenced by the presence of the surfactants, but not the nanoparticles. The order of the surfactants at the interface increases with increasing surfactant concentration, but is independent of nanoparticle concentration. Finally, the simulation has shown that surfactants can aggregate along the water–TCE interfaces, with and without the presence of nanoparticles.

Acknowledgments

We thank the Texas Tech High Performance Computing Center (HPCC) for computational resources. We are also grateful for the financial support from the National Science Foundation (CBET-0625191).

References

[1] Lin Y, Skaff H, Emrick T, Dinsmore A D and Russell T P 2003 *Science* **299** 226
[2] Lin Y, Skaff H, Böker A, Dinsmore A D, Emrick T and Russell T P 2003 *J. Am. Chem. Soc.* **125** 12690
[3] Stancik E J and Fuller G G 2004 *Langmuir* **20** 4805
[4] Melle S, Lask M and Fuller G G 2005 *Langmuir* **21** 2158
[5] Xu H, Melle S, Golemanov K and Fuller G G 2005 *Langmuir* **21** 10016
[6] Dinsmore A D, Hsu M F, Nikolaides M G, Marquez M, Bausch A R and Weitz D A 2002 *Science* **298** 1006
[7] Horozov T S, Aveyard R, Clint J H and Neumann B 2005 *Langmuir* **21** 2330
[8] Kralchevsky P A, Ivanov I B, Ananthapadmanabhan K P and Lips A 2005 *Langmuir* **21** 50
[9] Dickson J L, Binks B P and Johnston K P 2004 *Langmuir* **20** 7976
[10] Saleh N, Sarbu T, Sirk K, Lowry G V, Matyjaszewski K and Tilton R D 2005 *Langmuir* **21** 9873
[11] Tarimala S and Dai L L 2004 *Langmuir* **20** 3492
[12] Dai L L, Sharma R and Wu C Y 2005 *Langmuir* **21** 2641
[13] Luo M X, Mazyar O A, Zhu Q, Vaughn M W, Hase W L and Dai L L 2006 *Langmuir* **22** 6385
[14] Pillai V, Kanicky J R and Shah D O 1999 *Handbook of Microemulsion Science and Technology* (New York: Dekker)
[15] Kokal S 2005 *SPE Production Facilities* **20** 5
[16] Benjamin I 1997 *Annu. Rev. Phys. Chem.* **48** 407
[17] Senapati S and Berkowitz M L 2001 *Phys. Rev. Lett.* **87** 176101
[18] Moreira N H and Skaf M S 2004 *Prog. Colloid Polym. Sci.* **128** 81
[19] Zhang Y H, Feller S E, Brooks B R and Pastor R W 1995 *J. Chem. Phys.* **103** 10252
[20] Vanbuuren A R, Marrink S J and Berendsen H J C 1993 *J. Phys. Chem.* **97** 92062
[21] Fernandes P A, Cordeiro M N D S and Gomes J A N F 1999 *J. Mol. Struct. Theochem.* **463** 151
[22] Benjamin I 1992 *J. Chem. Phys.* **97** 1432
[23] Dang L X 1999 *J. Chem. Phys.* **110** 10113
[24] Rivera J L, McCabe C and Cummings P T 2003 *Phys. Rev.* E **67** 011603
[25] Schweighofer K J, Essmann U and Berkowitz M 1997 *J. Phys. Chem.* B **101** 3793

[26] Dominguez H 2002 *J. Phys. Chem.* B **106** 5915
[27] Berendsen H J C, Vanderspoel D and Vandrunen R 1995 *Comput. Phys. Commun.* **91** 43
[28] Lindahl E, Hess B and Van der Spoel D 2001 *J. Mol. Model* **7** 306
[29] Van der Spoel D, Lindahl E, Hess B, Groenhof G, Mark A E and Berendsen H J C 2005 *J. Comput. Chem.* **26** 1701
[30] Zhu Q and Vaughn M W 2005 *J. Phys. Chem.* B **109** 1947
[31] van Gunsteren W F, Billeter S R, Eising A A, Hüenberger P H, Krüger P, Mark A E, Scott W R P and Tironi I G 1996 *Biomolecular Simulation: The GROMOS 96 Manual and User Guide* (Zürich: Verlag der Fachvereine)
[32] William C S, Hans C A, Peter H B and Wilson K R 1982 *J. Chem. Phys.* **76** 637
[33] Kennard E H 1963 *Kinetic Theory of Gases* (New York: McGraw-Hill) p 77
Fleagle R G and Businger J A 1963 *An Introduction to Atmospheric Physics* (New York: Academic) p 31
[34] Huang K 1963 *Statistical Mechanics* (New York: Wiley) p 72
Chapman S and Cowling T G 1953 *The Mathematical Theory of Non-Uniform Gases* (London: Cambridge University Press) p 72
[35] Berendsen H J C, Postma J P M, Gunsteren W F and Hermans J 1981 *Intermolecular Forces* (Dordrecht: Reidel)
[36] Berendsen H J C, Grigera J R and Straatsma T P 1987 *J. Phys. Chem.* **91** 6269
[37] Schuttelkopf A W and van Aalten D M F 2004 *Acta Crystallogr.* D **60** 1355
[38] Mazyar O A and Hase W L 2006 *J. Phys. Chem.* A **110** 526
[39] Schweighofer K J, Essmann U and Berkowitz M 1997 *J. Phys. Chem.* B **101** 10775
[40] Andersen H C 1980 *J. Chem. Phys.* **72** 2384
[41] Berendsen H J C, Postma J P M, van Gunsteren W F, DiNola A and Haak J R 1984 *J. Chem. Phys.* **81** 3684
[42] Humphrey W, Dalke A and Schulten K 1996 *J. Mol. Graphics* **14** 33
[43] Li Y, He X J, Cao X L, Shao Y H, Li Z Q and Dong F L 2005 *Mol. Simul.* **31** 1027
[44] Telo Da Gama M M and Gubbins K E 1986 *Mol. Phys.* **59** 227
[45] Dominguez H and Berkowitz M L 2000 *J. Phys. Chem.* B **104** 5302
[46] Gaines G L 1966 *Insoluble Monolayers at Liquid–Gas Interfaces* (New York: Wiley)
[47] Ravera F, Santini E, Loglio G, Ferrari M and Liggieri L 2006 *J. Phys. Chem.* B **110** 19543
[48] Morrow M R, Singh D, Lu D and Grant C W M 1993 *Biophys. J.* **64** 654
[49] Dong F L, Li Y and Zhang P 2004 *Chem. Phys. Lett.* **399** 215
[50] Messmer M C, Conboy J C and Richmond G L 1995 *J. Am Chem. Soc.* **117** 8039
[51] Conboy J C, Messmer M C and Richmond G L 1996 *J. Phys. Chem.* **100** 7617
[52] Nicolas J P 2003 *Biophys. J.* **85** 1377
[53] van Buuren A R, Tieleman D P, de Vlieg J and Berendsen H J C 1996 *Langmuir* **12** 2570
[54] Tikhonov A M, Patel H, Garde S and Schlossman M L 2006 *J. Phys. Chem.* B **110** 19093